Time-dependent jetting on the surface of thin moving liquid layer. Part 1. Theoretical analysis

K.A Shishmarev[1,2a)], **T.I. Khabakhpasheva**[1,b)], **A.A. Korobkin**[1,3,c)]

1. Lavrentyev Institute of Hydrodynamics, Novosibirsk, pr. Lavrentyeva 15, 630090, Russia
2. Altai State University, Barnaul, pr. Lenina 61, 656049, Russia
3. University of East Anglia, Norwich, NR4 7TJ, UK

a) Electronic mail: shishmarev.k@mail.ru
b) Electronic mail: tana@hydro.nsc.ru
c) Electronic mail: a.korobkin@uea.ac.uk

ABSTRACT

Unsteady two-dimensional problem of a thin liquid layer with prescribed time-dependent influx into the layer, position of the influx section , and the thickness of the liquid at this section is studied by methods of asymptotic analysis. The ratio of the rate of the liquid thickness variation at the influx section to the influx velocity plays a role of a small parameter of the problem . The influx parameters are such that the flow in the thin layer is inertia dominated, with gravity, surface tension and liquid viscosity being approximately negligible. Such flows were studied with respect to several applications, some of which are listed in the Introduction. One of the applications concerns with splashing during droplet impact onto a rigid substrate and related kinematic discontinuity propagating along the spray sheet, which is produced by the spreading droplet. This type of splashing was studied by Yarin and Weiss (1995) within a quasi-one-dimensional approach averaging the flow velocity over the layer thickness. We also start with the one-dimensional thin-layer approximation assuming the influx flow is accelerated. Such influx conditions lead to unbounded growth of the thickness of the liquid layer at a certain location and at a certain time instant within the one-dimensional approach. The present study recovers for the first time the structure of the flow close to this singularity using methods of asymptotic analysis. To this aim, the second-order outer solution, which is valid outside the region of the unbounded flow, is derived. The second-order outer solution is used to find proper stretched inner variables and the equations governing the inner flow at the leading order. It is shown that the inner free-surface flow in the stretched variables is two-dimensional, potential, non-linear and independent of any parameters of the original problem.

I. INTRODUCTION

The original motivation to study thin liquid layer flows with time-dependent influxes come from the configuration depicted in Fig. 1. In this two-dimensional problem, an elastic plate impacts obliquely onto a thin liquid layer. In the Cartesian coordinate system Oxy, the line $y = 0$ corresponds to the rigid bottom, and the line $y = h$ corresponds to the initial undisturbed position of the liquid free surface. An elastic plate initially touches the liquid free surface at a single point, which is taken as $x = 0$, $y = h$. Then the plate moves to the right and penetrates the liquid layer. The initial velocities of the plate, initial inclination angle of the plate and the elastic characteristics of the plate are given. The coupled problem of the plate deflection and the flow under the plate was studied in the leading order by Khabakhpasheva and Korobkin (2020a). See also a review of existing results and approaches for the problem of oblique impact by rigid and elastic bodies on shallow water in that paper. A thin layer approximation was used, which is valid for long plates impacting the liquid layer at small angle and with a horizontal speed being much greater than vertical speed of the plate. In this approximation, the flow under the plate does not depend on the flow in the wake behind the plate. In the present study, we are concerned with the flow in the wake behind the plate. This flow is investigated using the computed characteristics of the flow at the trailing edge of the plate or at the section, where the free surface separates from the lower surface of the plate, after the coupled problem for the region below the moving plate has been solved. It will be shown below that the flow in the wake can also be described within the thin layer approximation, as the flow under the plate. However, if the influx into the wake is accelerated, then this approximation predicts unbounded thickness of the liquid layer at some locations behind the plate. The present study is focused on such influx conditions and fine details of the flow at these special locations.

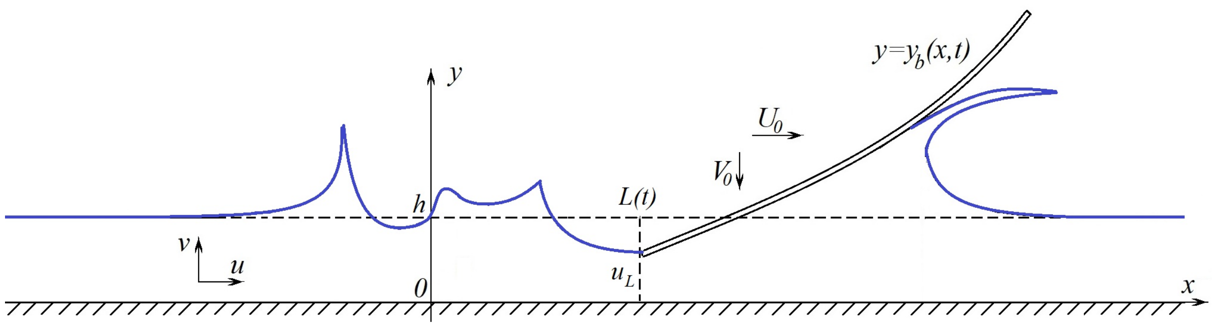

FIG. 1. Sketch of the flow in the wake behind a gliding elastic plate.

Flows in the wakes behind bodies impacting onto a liquid with high horizontal speeds are of practical interest because of possible water aeration in the wakes. Air entrainment during impacts of droplets onto a thin liquid layer, which is important for performance of some heat exchangers, was studied experimentally by Cherdantsev *et al.* (2017) and Hann *et al.* (2018). It was observed that the rate of the air entrainment during oblique droplet impacts is high and cannot be explained by the air-cushion effect, see Hicks and Purvis (2010, 2011). Possible mechanisms of the air entrainment by oblique droplet impact were modeled by Khabakhpasheva and Korobkin (2020a), who studied oblique impact of an elastic plate onto a thin liquid layer. The plate deflections were comparable with the thickness of the liquid layer. It was shown that air bubbles can be trapped in the liquid layer because of the plate leading edge rotation towards the liquid and elastic deflection of the plate, the jet formed at the leading edge of the wetted part of the plate, and the jets, which may be formed on the surface of the wake behind the plate, see Fig. 1. Experiments by Cherdantsev *et al.* (2017) showed that air bubbles are mainly entrained in the wake created behind an impacting droplet. Two-dimensional steady flows generated by bodies gliding along a free surface were studied by Semenov and Wu (2013) including the gravity effects. See also relevant studies and results by Yoon and Semenov (2011) and Faltinsen and Semenov (2008). Martinez-Legazpi *et al.* (2015) studied three-dimensional wake behind a high-speed vessel experimentally, numerically and theoretically, in order to explain high level of water aeration in such wakes.

We shall investigate evolution of the wake for the configuration depicted in Fig. 1. Khabakhpasheva and Korobkin (2020a) obtained that the speed of the flow at the entrance to the wake, $x = L(t)$, which is the trailing edge of the plate in Fig. 1, is zero initially, then becomes negative with increasing magnitude which exceeds the horizontal speed of the plate, see Fig. 3(d) in that paper, where the dimensionless speed of the flow at the inlet to the wake is shown by blue line. This implies that the liquid is injected into the wake from under the plate during the early stage of the oblique impact by the elastic plate. Later the flow speed at the entrance to the wake becomes positive. The flow into the wake is accelerated at the first stage and then decelerated. Within the thin layer inertia-dominated approximation, such time variation of the injection speed leads to a gradient catastrophe, which is an infinite gradient of the flow in the wake developed from a smooth input. Unbounded gradient of the flow results in unbounded increase of the thickness of the liquid layer, which can be interpreted as jetting from the surface of the liquid layer or splashing.

This mechanism of splashing was studied by Pegg *et al.* (2018) in the axisymmetric problem of droplet impact onto an elastic plate of small radius, see Fig. 2(a), and by Khabakhpasheva and Korobkin (2020b) in the problem of droplet impact onto a vibrating plate, see Fig. 2(b). The elastic plate starts to vibrate after it is completely wetted and the impact pressures are not very high in the problem studied by Pegg *et al.* (2018). These vibrations lead to oscillations of the wetted area expansion and oscillations of the flow speed into the spray sheet. Parameters of the problem were obtained such that the plate oscillations result in unbounded increase of the thickness of the spray sheet, see Fig. 2(a), which was interpreted as splashing. The same mechanism of splashing was discovered in the axisymmetric problem of droplet impact onto vibrating rigid plate, see Khabakhpasheva and Korobkin (2016, 2020b). Variations of the amplitude and frequency of the plate vibration allow us to control splashing making the splashing close to the periphery of the wetted part of the plate, which may lead to entrapping the air in front of the advancing free surface of the droplet, see Fig. 2(b). It was shown that only forced vibration of the plate causes splashing. The gravity, surface tension and the liquid viscosity were neglected in both problems. Places and times of splashing were calculated. However, it was not clear how the jetting from the surface of the spray sheet develops, what are the jet thickness and its speed. Deeper analysis of the local flow near the place of the splashing was required. This type of splashing can be also detected in free liquid jets with oscillations of the flow speed at the entrance to the jet, see Fig. 2(c). The effect of these kinematic waves, which are caused by pulsation of the entry jet speed, on jet break down was studied by Meier *et al.* (1992). Note that Fig. 2(a-g) show only sketches of the processes but not their dynamics.

Yarin and Weiss (1995) studied splashing during droplet impact onto a dry and rigid substrate, see Fig. 2(d). They argued that "the splashing threshold corresponds to the onset of a velocity discontinuity propagating over the liquid layer on the wall. This discontinuity shows several aspects of a shock."A simplified quasi-one-dimensional approach with averaged velocity of the flow across the layer thickness including the surfac by e tension effects and excluding gravity and viscous effects was used. The unsteady one-dimensional equations of the flow were solved for a given initial distribution of the flow velocity in the liquid layer. This initial distribution was represented by a finite hump, see Fig. 18 in their paper, with "a sharp decrease"of the velocity at the ends of the hump. This problem is similar theoretically to the problem of droplet splashing caused by a gradient catastrophe of the flow in the layer, where input distributions are smooth. The model developed and studied by Yarin and Weiss (1995) "predicts the existence of a new type of kinematic discontinuity wave, namely a discontinuity in the velocity and film-thickness distributions. This discontinuity shows many aspects of a shock wave, but also propagates in an incompressible liquid. The discontinuity has a sink of mass at its front, which corresponds to the emergence of a thin liquid sheet parallel to the discontinuity front and virtually normal to the film on the wall."

Stumpf *et al.* (2021) studied drop impact onto a thin viscous film with focus on parameters of the corona, see Fig. 2(e). The liquid in the viscous film and the liquid in the droplet did not mix during the impact. This problem is similar to the problem studied by Yarin and Weiss (1995), however, there are several new effects in the problem of droplet impact onto a viscous film. One of them is the flow of the viscous film under the spreading droplet with the possibility that some liquid from the

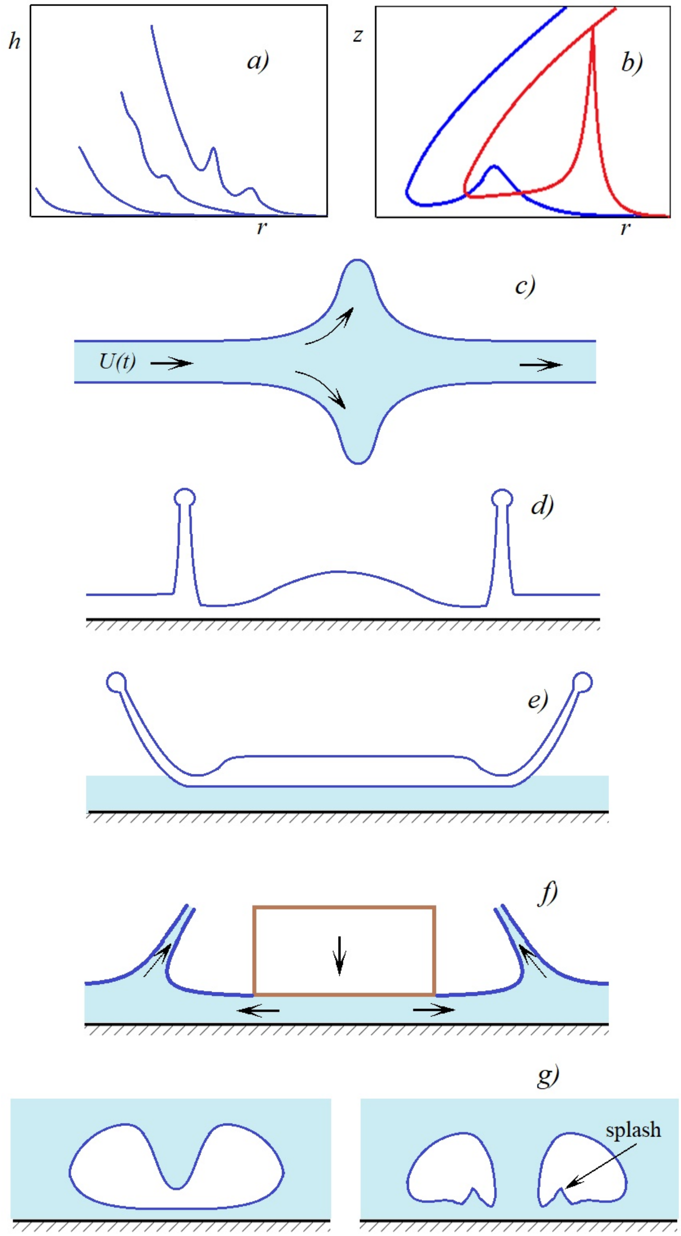

FIG. 2. Sketch of the spray sheet thickness at different time instants in the axisymmetric problem of spherical droplet impact onto (a) a small elastic circular plate mounted into a rigid substrate, and (b) a vibrating rigid plate. Here $h(r,t)$ is the spray sheet thickness, r is the radial coordinate, $r = 0$ at the point of the initial impact, z is the vertical coordinate, $z = 0$ on the vibrating plate. (c) Kinematic waves caused by pulsation of the jet speed. Splashing by drop impact onto dry (d) and wet (e) substrates. (f) Flat plate impact onto a thin liquid layer. (g) Collapse of a bubble near a rigid wall with splashes. More details about the dynamics of the processes depicted in this figure can be found in the papers cited in the text.

viscous film enters the corona. It is expected that regimes of such impact and splashing depend on relative velocity of the droplet spreading over the viscous film and the velocity of this viscous film, which is caused by squeezing the viscous layer by the impacting droplet. Replacing the droplet with a rigid plate and focusing on the flow in the thin inviscid layer outside the plate, see Fig. 2(f), one arrives at the problem studied by Korobkin (1999). Initial speed of the outflow from under the plate was non-zero with the thin liquid layer outside the plate being initially at rest. This discontinuity resulted in formation of jets moving from the plate and inclined to the initial surface of the liquid layer. The motion of the jet root and the jet thickness were calculated using the conservation laws of mass and impulse. If the plate moves at a constant speed, the jets are inclined towards the plate at the angle 45 degrees, which well corresponds to the angle measured in experiments with a heavy box falling onto shallow water by Bukreev and Gusev (1996). Such inclined jets on the surface of the liquid layer can trap air when the jets fall down due to gravity. The asymptotic model of sudden plate impact onto shallow water by Korobkin (1999) was confirmed experimentally by Kang *et al.* (2008).

Korobkin (1999) studied two-dimensional and three dimensional problems of impact by a flat plate onto a thin liquid layer, as well as impacts by an elastic plate. However, the original motivation of this paper came from the experiments and analysis of a bubble collapse near a rigid wall by Tong *et al.* (1999). A sketch of the bubble collapse near a rigid wall is shown in Fig. 2(g). Note the splash on the thin film between the collapsing bubble and the wall. It was argued that the pressure on the wall under these splashes could be higher than the pressure at the centre of impact. In section 7 of Korobkin (1999), it was shown that in the problem of rigid plate impact onto a thin liquid layer the pressure always is maximum at the centre of the plate. However, for the plate penetrating the liquid layer with deceleration, the pressure in the splash roots can be higher than at the plate centre.

In contrast to the problem studied by Korobkin (1999), in the present paper, we investigate the flow of a thin liquid layer caused by a given smooth inflow of the liquid through a section, which moves at a given speed, see Fig. 1. For example, in the problem of oblique impact by an elastic plate onto a thin liquid layer of thickness h, we are given the x-coordinate, $x = L(t)$, of the point on the plate, position of which is described by equation $y = y_b(x, t)$, where the free surface of the wake separates from the plate, the distance of this separation point, $h - s(t)$, from the bottom of the liquid layer, and the averaged horizontal velocity of the flow at the entrance to the wake, $u(L(t), t) = u_L(t)$. Initially, $L(0) = 0$, $u_L(0) = 0$ and $s(0) = 0$ at $t = 0$. We assume that the speed of the separation point, $L'(t)$, and the speed of the liquid inflow into the wake, $u_L(t)$ if $u_L(t) < 0$, are of order of U, and the vertical speed of the separation point, $s'(t)$, is of order of V, where U and V are initial horizontal and vertical velocities of the plate with $V/U = \varepsilon$ being a small parameter of the problem. In this paper, the speed scales U and V and other parameters of the flow in the wake are such that the flow is governed by the liquid inertia with gravity and surface tension playing secondary roles, and liquid viscosity being negligible. The leading-order solution of this problem was studied by Shishmarev *et al* (2020) using the method of characteristics for smooth influx data from the paper by Khabakhpasheva and Korobkin (2020a).

Other ranges of the inflow parameters will be investigated in Part 3 of this study. In particular, the regime with the wake flow being governed at the leading order by liquid inertia and the surface tension, as in the study by Yarin and Weiss (1995), will be described. Edwards *et al* (2008) investigated unsteady impact of two thin liquid layers at a high Froude number Fr using the methods of asymptotic analysis. In the paper by Edwards *et al* (2008), the singularity of the solution at $Fr = \infty$ was resolved assuming that the gravity effects provide a major contribution to the dynamics of the flow near the singularity.

To obtain the conditions of inertia dominated flow in the wake, we introduce dimensionless variables, identify parameters responsible for different effects, and construct a formal second-order asymptotic solution of the hydrodynamic problem with free surface in the wake as $\varepsilon \to 0$. This asymptotic solution is not uniformly valid for some inflow conditions at $x = L(t)$. Such cases will be identified and the leading order solutions localized in time and space near the singularities of the outer solution will be obtained. These local solutions describe jetting in the wake, which may lead potentially to entrapping air into the liquid layer behind a planning plate. Note that the flow in the wake, which is of main concern in this paper, depends only on the smooth functions $L(t)$, $u_L(t)$ and $s(t)$, and does not depend on both the details of the flow in $x > L(t)$ and the body motion. Therefore, the present analysis is valid also for any two-dimensional thin-layer flows with a time-varying inflow speed and a time-varying position of the flow inlet.

The second-order terms in the solution in the wake as $\varepsilon \to 0$ provide small contributions to the leading order solution everywhere in the wake except a small region, where the gradient catastrophe occurs. The second-order solution is needed to find the dimensions of the region, where the second-order terms of the solution are of the same order as the leading order terms and more detailed analysis of the flow is required, as well as the inner coordinates in this region. It will be shown that the inner coordinates are related to the original variables x, y and t by complicated relations, which would be difficult to obtain using only physical reasoning. The flow in the wake at the leading order as $\varepsilon \to 0$ is one-dimensional, unsteady and nonlinear. The flow in the inner region at the leading order in stretched variables is two-dimensional, potential, non-linear and unsteady with unknown in advance free surface, but independent of any parameters of the original problem. The forcing comes to this universal problem through matching conditions in the far field. Therefore, we will derive and present this universal problem without any parameters in it, which governs jetting from the surface of a thin liquid layer for smooth inflow conditions.

The general formulation of the problem will be presented and discussed in section II. The range of the parameters of the problem, where the flow in the wake is inertia dominated at the leading order as $\varepsilon \to 0$, will be obtained. The asymptotic analysis of the problem with the small parameter ε will be performed in section III. The leading order solution and the first order corrections to it as $\varepsilon \to 0$ will be derived. This second order outer solution will be analysed in terms of its validity when $u_L'(t)$ is negative, which implies that the inflow into the wake is accelerated. The conditions of the gradient catastrophe will be obtained. The time and place, when and where this catastrophe with unbounded growth of the wake surface elevation occurs, will be determined and the behaviour of the outer second-order solution near the catastrophe conditions will be analysed in section IV. The model governing the local flow at the leading order and describing the jetting from the wake surface will be derived and studied in section V. The conclusions are drawn in section VI together with short introductions of Part 2 and 3 of this study.

II. FORMULATION OF THE PROBLEM

In general, a two-dimensional flow of incompressible liquid in the wake, $x < L(t)$, $0 < y < \eta(x,t)$, is governed by the Navier-Stokes equations,

$$\frac{\partial u}{\partial x} + \frac{\partial v}{\partial y} = 0, \qquad \frac{\mathrm{D}u}{\mathrm{D}t} = -\frac{1}{\rho}\frac{\partial p}{\partial x} + \nu\nabla^2 u, \qquad \frac{\mathrm{D}v}{\mathrm{D}t} = -\frac{1}{\rho}\frac{\partial p}{\partial y} + \nu\nabla^2 v, \tag{1}$$

where the equation $y = \eta(x,t)$ describes the elevation of the liquid free surfaces, $u(x,y,t)$ and $v(x,y,t)$ are the horizontal and vertical components of the flow velocity correspondingly, ρ is the liquid density, ν is the kinematic viscosity of the liquid, and $p(x,y,t)$ is the hydrodynamic pressure. The total pressure is equal to $p(x,y,t)$ plus the hydrostatic pressure $\rho g(h-y)$, where g is the gravitational acceleration and h is the equilibrium thickness of the liquid. The flow vorticity,

$$\omega(x,y,t)=\frac{\partial v}{\partial x}-\frac{\partial u}{\partial y}, \tag{2}$$

satisfies the equation

$$\frac{\mathrm{D}\omega}{\mathrm{D}t}=\nu\nabla^2\omega. \tag{3}$$

In (1) and (3), $\mathrm{D}/\mathrm{D}t=\partial/\partial t+u\partial/\partial x+v\partial/\partial y$ is the material derivative, and $\nabla^2=\partial^2/\partial x^2+\partial^2/\partial y^2$ is the Laplacian.

Equations (1) and (3) are to be solved subject to the kinematic,

$$\frac{\partial\eta}{\partial t}+\frac{\partial\eta}{\partial x}u=v(x,\eta(x,t),t), \tag{4}$$

and dynamic,

$$\vec{\tau}\cdot P\vec{n}=0, \qquad \vec{n}\cdot P\vec{n}=\gamma æ, \tag{5}$$

boundary conditions on the liquid free surface, $y=\eta(x,t)$, $x<L(t)$. Here $P(x,y,t)$ is the stress tensor,

$$P=-(p+\rho g(h-y))\begin{pmatrix}1&0\\0&1\end{pmatrix}+2\rho\nu\begin{pmatrix}\frac{\partial u}{\partial x} & \frac{1}{2}\left(\frac{\partial u}{\partial y}+\frac{\partial v}{\partial x}\right)\\ \frac{1}{2}\left(\frac{\partial u}{\partial y}+\frac{\partial v}{\partial x}\right) & \frac{\partial v}{\partial y}\end{pmatrix}, \tag{6}$$

$\vec{n}$ and $\vec{\tau}$ are the normal and tangent unit vectors to the free surface,

$$\vec{n}=(-\eta_x,1)/R, \quad \vec{\tau}=(1,\eta_x)/R, \quad R=\sqrt{1+\eta_x^2}, \tag{7}$$

$æ(x,t)$ is the curvature of the free surface, $æ=\eta_{xx}/R^3$, and γ is the coefficient of surface tension. The dynamic conditions (5) imply that there are no both normal and tangential stresses on the free surface of the liquid.

On the bottom,

$$u=v=0 \qquad (y=0,\ x<L(t)). \tag{8}$$

At the entrance to the wake, $x=L(t)$, the following conditions are imposed

$$\eta(L(t),t)=h-s(t), \quad \omega(L(t),y,t)=0, \quad \int_0^{h-s(t)}u(L(t),y,t)\mathrm{d}y=u_L(t)(h-s(t)), \tag{9}$$

where $0<y<h-s(t)$. The functions $u_L(t)$, $s(t)$ and $L(t)$ are prescribed in the present study. Note that imposing the vorticity at the entrance to the wake as zero is an approximation, which follows from minor role of the liquid viscosity under the plate, see Khabakhpasheva and Korobkin (2020a). Note that the flux into the wake is prescribed in (9) but not the velocity distribution at the entrance to the wake. Conditions (9) are correct within the second order thin layer approximation employed in the present study. Higher order approximations and other ranges of the flow parameters would require more refined inflow conditions including, in particular, the vertical component of the flow velocity at the entrance to the wake. The initial conditions for the problem (1)-(8) are

$$u(x,y,0)=0, \quad v(x,y,0)=0, \quad p(x,y,0)=0, \quad \eta(x,0)=h, \quad \omega(x,y,0)=0 \quad (x<0). \tag{10}$$

The flow in the wake decays as $x\to-\infty$.

The formulated problem is investigated in dimensionless variables. The thickness of the liquid layer h is taken as the scale of the vertical coordinate y and the free-surface elevation η. The scale

U of the influx speed $u_L(t)$ is taken as the scale of the horizontal velocity of the flow in the liquid layer. The scale V of the time variation of the wake thickness at the inlet, $s'(t)$, is taken as the scale of the vertical velocity of the flow in the liquid layer. The ratio $\varepsilon = V/U$ is a dimensionless small parameter of the problem. The scale of the horizontal coordinate x is selected as $h\varepsilon^{-1}$ to keep the continuity equation non-trivial in the dimensionless variables when $\varepsilon \to 0$. Dimensionless variables are denoted with tilde and are introduced by the following relations,

$$u = U\tilde{u}(\tilde{x}, \tilde{y}, \tilde{t}), \quad v = V\tilde{v}(\tilde{x}, \tilde{y}, \tilde{t}), \quad x = h\varepsilon^{-1}\tilde{x}, \quad y = h\tilde{y}, \quad \eta = h\tilde{\eta}(\tilde{x}, \tilde{t}), \quad t = \frac{h\tilde{t}}{V}, \tag{11}$$

$$u_L(t) = U\tilde{u}_L(\tilde{t}), \quad L(t) = h\varepsilon^{-1}\tilde{L}(\tilde{t}), \quad s(t) = h\tilde{s}(\tilde{t}), \quad \omega = \frac{U}{h}\tilde{\omega}(\tilde{x}, \tilde{y}, \tilde{t}), \quad p = \rho V^2\tilde{p}(\tilde{x}, \tilde{y}, \tilde{t}).$$

The material derivative in the dimensionless variables and the dimensionless vorticity read

$$\frac{\mathrm{D}}{\mathrm{D}t} = \frac{V}{h}\frac{\tilde{\mathrm{D}}}{\tilde{\mathrm{D}}t}, \quad \frac{\tilde{\mathrm{D}}}{\tilde{\mathrm{D}}t} = \frac{\partial}{\partial\tilde{t}} + \tilde{u}\frac{\partial}{\partial\tilde{x}} + \tilde{v}\frac{\partial}{\partial\tilde{y}}, \qquad \tilde{\omega}(\tilde{x}, \tilde{y}, \tilde{t}) = -\frac{\partial\tilde{u}}{\partial\tilde{y}} + \varepsilon^2\frac{\partial\tilde{v}}{\partial\tilde{x}}. \tag{12}$$

Equations (1) and (3) in the dimensionless variables have the forms

$$\frac{\tilde{\mathrm{D}}\tilde{u}}{\tilde{\mathrm{D}}\tilde{t}} = -\varepsilon^2\frac{\partial\tilde{p}}{\partial\tilde{x}} + \frac{1}{Re}\left(\frac{\partial^2\tilde{u}}{\partial\tilde{y}^2} + \varepsilon^2\frac{\partial^2\tilde{u}}{\partial\tilde{x}^2}\right), \quad \frac{\tilde{\mathrm{D}}\tilde{v}}{\tilde{\mathrm{D}}\tilde{t}} = -\frac{\partial\tilde{p}}{\partial\tilde{y}} + \frac{1}{Re}\left(\frac{\partial^2\tilde{v}}{\partial\tilde{y}^2} + \varepsilon^2\frac{\partial^2\tilde{v}}{\partial\tilde{x}^2}\right), \tag{13}$$

$$\frac{\partial\tilde{u}}{\partial\tilde{x}} + \frac{\partial\tilde{v}}{\partial\tilde{y}} = 0, \qquad \frac{\tilde{\mathrm{D}}\tilde{\omega}}{\tilde{\mathrm{D}}\tilde{t}} = \frac{1}{Re}\left(\frac{\partial^2\tilde{\omega}}{\partial\tilde{y}^2} + \varepsilon^2\frac{\partial^2\tilde{\omega}}{\partial\tilde{x}^2}\right), \tag{14}$$

where $Re = hV/\nu$ is the Reynolds number and $0 < \tilde{y} < \tilde{\eta}(\tilde{x}, \tilde{t})$, $\tilde{x} < \tilde{L}(\tilde{t})$. The boundary conditions (4) and (5) on the free surface, $\tilde{y} = \tilde{\eta}(\tilde{x}, \tilde{t})$, where $\tilde{x} < \tilde{L}(\tilde{t})$, take the forms

$$\frac{\partial\tilde{\eta}}{\partial\tilde{t}} + \frac{\partial\tilde{\eta}}{\partial\tilde{x}}\tilde{u} = \tilde{v}, \qquad \tilde{\omega} = 2\varepsilon^2\left(\frac{\partial\tilde{v}}{\partial\tilde{x}} - \frac{2}{\tilde{R}_-^2}\frac{\partial\tilde{u}}{\partial\tilde{x}}\frac{\partial\tilde{\eta}}{\partial\tilde{x}}\right), \tag{15}$$

$$\tilde{p} = \frac{1}{Fr^2}(\tilde{\eta} - 1) - \frac{1}{We\tilde{R}_+^3}\frac{\partial^2\tilde{\eta}}{\partial\tilde{x}^2} - \frac{2}{Re}\frac{\partial\tilde{u}}{\partial\tilde{x}}\frac{\tilde{R}_+^2}{\tilde{R}_-^2}, \tag{16}$$

where $Fr = V/\sqrt{gh}$ is the Froude number, $We = \rho hU^2/\gamma$ is the Weber number, $\tilde{R}_+ = \sqrt{1 + (\varepsilon\partial\tilde{\eta}/\partial\tilde{x})^2}$, and $\tilde{R}_- = \sqrt{1 - (\varepsilon\partial\tilde{\eta}/\partial\tilde{x})^2}$, see Appendix A for more details. The boundary conditions (8) on the bottom, at the entrance to the wake (9) and the initial conditions (10) keep their forms in the dimensionless variables with adding tilde for all variables and replacing h by 1.

The formulated boundary value problem (8)-(10), (13)-(16) is investigated using methods of asymptotic analysis assuming that $\varepsilon \ll 1$, $\varepsilon^2 Re \gg 1$, $\varepsilon^2 We \gg 1$ and $\varepsilon Fr \gg 1$. For example, Khabakhpasheva and Korobkin (2020a) performed calculations for an aluminium plate of length 10 cm and thickness 2 mm impacting on the water layer with depth 2 cm. The edges of the plate were free of stresses and shear forces. The rigid and elastic motions of the plate were calculated as part of the solution. The initial inclination angle of the plate was 3°, 6° and 10°. The vertical initial speed of the plate was 5 m/s in all calculations. The initial horizontal velocity of the plate was 5, 15 and 25 m/s. The calculated vertical velocity of the plate near its trailing edge reduces shortly after the impact to zero, see Fig. 3(b) in Khabakhpasheva and Korobkin (2020a). Then the trailing edge of the plate starts exiting from the liquid layer. For those calculations, $V = 5$ m/s, $U = 25$ m/s, $h = 0.02$ m, $\gamma = 72.53 \cdot 10^{-3}$ N/m, $\nu = 10^{-6}$ m^2/s, $g = 9.81$ m/s^2, and $\rho = 1000$

kg/m^3, which give $\varepsilon = 0.2$, $Fr = 11.3$, $We = 1.7 \cdot 10^5$, and $Re = 10^5$. Therefore, our assumptions that the gravity, surface tension and the liquid viscosity can be neglected at the leading order in the main part of the wake are approximately valid for these conditions of the flow in the wake. Note that ε in the calculations mentioned above is not very small. However, we can think about other impact conditions, for which the assumption $\varepsilon \ll 1$ is well justified. For example, in the experiments with droplet impacts onto a thin liquid layer by Cherdantsev et all.(2017), the horizontal speed of the droplets was estimated as 30 m/s and their vertical speed at the impact with the liquid layer as 1 m/s, which gives $\varepsilon = 1/30$. Other regimes of the thin layer flows will be studied in Part 3. Note that we arrive at the model studied by Yarin and Weiss (1995) if $We = O(1)$.

The assumptions $\varepsilon \ll 1$, $\varepsilon^2 Re \gg 1$, $\varepsilon^2 We \gg 1$ and $\varepsilon Fr \gg 1$ imply that viscosity, surface tension and gravity give contributions to the terms in the formulated problem which are higher than $O(\varepsilon^2)$. Neglecting terms of order higher than $O(\varepsilon^2)$, we conclude that the flow vorticity is zero, and the flow in the wake is non-linear and potential with unknown in advance shape of the free surface within this approximation. The condition (15) describes the vorticity generation in the viscous boundary layer on the free surface. This condition can be approximately dropped together with the condition of no-slip on the bottom because they affect the flow only near the boundary of the wake but not in the main part of it.

We arrive at the wake problem for potential flow of inviscid liquid without gravity and surface tension. Dropping tilde and all terms of order higher than ε^2, we obtain the following equations,

$$\frac{\mathrm{D}u}{\mathrm{D}t} = -\varepsilon^2 \frac{\partial p}{\partial x}, \quad \frac{\mathrm{D}v}{\mathrm{D}t} = -\frac{\partial p}{\partial y}, \quad \frac{\partial u}{\partial x} + \frac{\partial v}{\partial y} = 0, \quad \frac{\partial u}{\partial y} = \varepsilon^2 \frac{\partial v}{\partial x}, \quad (0 < y < \eta(x,t),\ x < L(t)), \tag{17}$$

$$\frac{\partial \eta}{\partial t} + \frac{\partial \eta}{\partial x} u = v, \quad p = 0 \qquad (y = \eta(x,t), \quad x < L(t)), \tag{18}$$

$$v = 0 \qquad (y = 0, \quad x < L(t)), \tag{19}$$

$$\eta(L(t),t) = 1 - s(t), \qquad \int_0^{1-s(t)} u(L(t),y,t)\mathrm{d}y = u_L(t)(1 - s(t)), \tag{20}$$

$$u(x,y,0) = v(x,y,0) = p(x,y,0) = 0, \qquad \eta(x,0) = 1. \tag{21}$$

In the problem (17) - (21), $u_L(t)$, $s(t)$ and $L(t)$ are given functions of time.

The solution of the problem (17) - (21) as $\varepsilon \to 0$ is sought in the form

$$\begin{aligned} u(x,y,t) &= u_0(x,t) + \varepsilon^2 u_1(x,y,t) + O(\varepsilon^4), \\ v(x,y,t) &= v_0(x,y,t) + \varepsilon^2 v_1(x,y,t) + O(\varepsilon^4), \\ p(x,y,t) &= p_0(x,y,t) + \varepsilon^2 p_1(x,y,t) + O(\varepsilon^4), \\ \eta(x,t) &= \eta_0(x,t) + \varepsilon^2 \eta_1(x,t) + O(\varepsilon^4). \end{aligned} \tag{22}$$

Substituting the asymptotic expansions (22) in equations (17)-(21), we obtain in the leading order,

$$u_{0t} + u_0 u_{0x} = 0, \quad v_{0y} = -u_{0x} \quad (x < L(t)), \qquad u_0(L(t),t) = u_L(t), \quad v_0(x,0,t) = 0, \tag{23}$$

$$\eta_{0t} + \eta_{0x} u_0 + \eta_0 u_{0x} = 0 \quad (x < L(t)), \quad \eta_0(L(t),t) = 1 - s(t), \tag{24}$$

$$p_{0y} = -2y u_{0x}^2(x,t), \quad p_0(x,\eta_0(x,t),t) = 0. \tag{25}$$

Equations (17) -(21) in the second order provide

$$u_{1t} + u_0 u_{1x} + u_1 u_{0x} + v_0 u_{1y} = -p_{0x}, \qquad \int_0^{1-s(t)} u_1(L(t),y,t)\mathrm{d}y = 0, \tag{26}$$

$$v_{1y} = -u_{1x}, \quad v_1(x,0,t) = 0, \tag{27}$$

$$\eta_{1t} + (u_0\eta_1)_x = -\eta_{0x}u_1(x,\eta_0(x,t),t) + v_1(x,\eta_0(x,t),t), \quad \eta_1(L(t),t) = 0. \tag{28}$$

$$-p_{1y} = v_{1t} + u_0 v_{1x} + u_1 v_{0x} + v_0 v_{1y} + v_1 v_{0y}, \quad p_1(x,\eta_0(x,t),t) = -p_{0y}(x,\eta_0,t)\eta_1(x,t), \tag{29}$$

$$u_{1y} = v_{0x}, \tag{30}$$

where $x < L(t)$ and $0 < y < \eta_0(x,t)$. In equations (23)-(30) and below , lower indexes x, y and t correspond to partial derivatives with respect to x, y and t. For example, $u_{0t} = \partial u_0/\partial t$, $\eta_{0x} = \partial\eta_0/\partial x$ and $p_{0y} = \partial p_0/\partial y$. We shall determine the leading order approximations of the unknown functions solving (23)-(25), investigate conditions of applicability of this solution, and determine the second order terms of the solution solving (26)-(30).

III. LEADING-ORDER FLOW IN THE WAKE

Equation (23) implies that a liquid particle entering the wake at time τ through section $x = L(\tau)$ moves at constant velocity $u_L(\tau)$. By time t, $t > \tau$, this particle travels the distance $x = L(\tau) + u_L(\tau)(t-\tau)$. This gives the solution of (23) in parametric form,

$$x = x(\tau,t) = L(\tau) + u_L(\tau)(t-\tau) \quad (t > \tau), \tag{31}$$

$$u_0(x,t) = u_0(x(\tau,t),t) = u_L(\tau). \tag{32}$$

The leading order horizontal velocity $u_0(x,t)$ in the wake is always bounded for bounded inflow velocity $u_L(t)$. However, the leading order vertical velocity, $v_0(x,y,t) = -yu_{0x}(x,t)$, in the wake can be unbounded. By differentiating (32) with respect to τ, we find

$$u_{0x}(x,t) = \frac{u'_L(\tau)}{x_\tau(\tau,t)}, \tag{33}$$

where the derivative $x_\tau(\tau,t)$ is obtained from (31),

$$x_\tau(\tau,t) = L'(\tau) - u_L(\tau) + u'_L(\tau)(t-\tau).$$

A prime stands for the derivative with respect to τ. Here $u'_L(\tau)$ is the acceleration of the flow at $x = L(\tau)$, $u_L(\tau)$ is positive for the flow from left to right, see Fig. 1. The function $u_R(\tau) = L'(\tau) - u_L(\tau)$ is the velocity of the flow into the wake with respect to the moving entrance, $x = L(\tau)$. The relative velocity $u_R(\tau)$ is positive if the liquid enters the wake through $x = L(\tau)$. We assume in the present study that $u_R(t)$ is positive for $t > 0$. Then

$$x_\tau(x,t) = u_R(\tau) + u'_L(\tau)(t-\tau), \tag{34}$$

where $t - \tau \geq 0$ and $u_R(\tau) \geq 0$. The derivative (34) can be zero and, therefore, the derivative u_{0x} in (33) and the vertical velocity $v_0(x,t) = -yu_{0x}(x,t)$ are unbounded at $t = \tau - u_R(\tau)/u'_L(\tau)$ if $u'_L(\tau) < 0$. We assume that this inequality is satisfied at some interval of time.

For given functions $L(t)$ and $u_L(t)$, we define $t = t_c(\tau) = \tau - u_R(\tau)/u'_L(\tau)$ and denote the minimum positive value of this function as t_*. The value of τ, at which this minimum is achieved, is denoted by τ_*. We have $t_* = t_c(\tau_*)$. The value $x(\tau_*, t_*)$ is denoted by x_*. We conclude that the vertical velocity in the wake becomes unbounded for the first time at $t = t_*$ at the distance x_* from the origin. This is possible only if the flow into the wake is accelerated. Note that the leading order pressure (25) is also unbounded at $x = x_*$ and $t = t_*$.

The thickness of the liquid layer is governed by equation (24). We obtain, see Shishmarev Conf series (2020),

$$\eta_0(x,t) = \frac{Q(\tau)}{x_\tau(\tau,t)}, \tag{35}$$

where $Q(\tau) = [1 - s(\tau)]u_R(\tau)$ is the flux of the flow into the wake. Substituting (33) and (35) in (25), we obtain the leading-order pressure in the wake,

$$p_0(x,y,t) = \Big(\frac{u_L'(\tau)}{x_\tau}\Big)^2 \Big\{\Big(\frac{Q(\tau)}{x_\tau}\Big)^2 - y^2\Big\} \quad (0 < y < \eta_0(x,t), x < L(t)). \tag{36}$$

Note that the leading-order pressure grows as $O(x_\tau^{-4}(\tau,t))$ when $\tau \to \tau_*$, $t \to t_*$ and, as a result, $x_\tau(\tau,t) \to 0$.

IV. SECOND-ORDER TERMS OF THE SOLUTION IN THE WAKE

For a function $f(x,y,t)$ of x, y and t, it is convenient to introduce a new function $\bar{f}(\tau,y,t) = f(x(\tau,t),y,t)$, where $x(\tau,t)$ is given by (31). Derivatives of $f(x,y,t)$ and $\bar{f}(\tau,y,t)$ are related by

$$\frac{\partial f}{\partial x} = \frac{1}{x_\tau(\tau,t)}\frac{\partial \bar{f}}{\partial \tau}, \qquad \frac{\partial f}{\partial t} + u_0(x,t)\frac{\partial f}{\partial x} = \frac{\partial \bar{f}}{\partial t}, \qquad \frac{\partial f}{\partial y} = \frac{\partial \bar{f}}{\partial y}. \tag{37}$$

By using (25), (30) and (33)-(36), equation (26), can be written as

$$\frac{\partial \bar{u}_1}{\partial t} + u_{0x}\bar{u}_1 = -3\frac{u_L' a_4(\tau)}{x_\tau^5} + 4\frac{u_L' Q^2 \mu}{x_\tau^6} - y^2\frac{\mu u_L'}{x_\tau^4}, \tag{38}$$

where $t > \tau$, $a_4(\tau) = [u_L'(Q^2)' - 2u_L'' Q^2]/3$, and $\mu(\tau) = u_L'(u_R' - u_L') - u_L'' u_R$. The right-hand side in (38) depends on time t only through the derivative $x_\tau(\tau,t)$. Note that

$$u_L' x_{\tau\tau} = \mu(\tau) + u_L'' x_\tau(\tau,t). \tag{39}$$

To find the general solution to the differential equation (38), we notice that

$$\left[\frac{\partial}{\partial t} + \frac{u_L'(\tau)}{x_\tau(\tau,t)}\right]\frac{1}{x_\tau^n(\tau,t)} = \frac{(1-n)u_L'(\tau)}{x_\tau^{n+1}(\tau,t)}, \tag{40}$$

which gives

$$\bar{u}_1(\tau,y,t) = \frac{a_4(\tau)}{x_\tau^4} - \frac{Q^2\mu}{x_\tau^5} + y^2\frac{\mu}{2x_\tau^3} + \frac{C_1(\tau)}{x_\tau}. \tag{41}$$

The last term in (41) is the general solution of the homogeneous equation (38), see (40). The function $C_1(\tau)$ is determined using the condition at $x = L(t)$, see (26), $C_1(\tau) = (5\mu Q^2 - 6a_4 u_R)/(6u_R^4)$.

Equations (27), (37) and (41) provide the second-order vertical velocity of the flow in the wake,

$$\bar{v}_1(\tau,y,t) = y\Big(-\frac{5Q^2\mu^2}{u_L'}\frac{1}{x_\tau^7} - \Big[\frac{23}{3}\mu Q^2\frac{u_L''}{u_L'} - \frac{14}{3}\mu Q Q' - Q^2\mu'\Big]\frac{1}{x_\tau^6} - \Big[a_4' - 4a_4\frac{u_L''}{u_L'}\Big]\frac{1}{x_\tau^5} +$$

$$\frac{C_1\mu}{u_L'}\frac{1}{x_\tau^3} - \Big[C_1' - \frac{C_1 u_L''}{u_L'}\Big]\frac{1}{x_\tau^2}\Big) + y^3\Big(\frac{\mu^2}{2u_L'}\frac{1}{x_\tau^5} - \Big[\frac{1}{6}\mu' - \frac{\mu u_L''}{2u_L'}\Big]\frac{1}{x_\tau^4}\Big). \tag{42}$$

Using (37) one can present equation (28) for the second-order free-surface elevation as

$$\frac{\partial \bar{\eta}_1}{\partial t} + u_{0x}\bar{\eta}_1 = -\eta_{0x}\bar{u}_1(\tau, \eta_0, t) + \bar{v}_1(\tau, \eta_0, t), \tag{43}$$

where

$$\eta_{0x} = \frac{Q\mu}{u_L'}\frac{1}{x_\tau^3} + \Big(Q' - Q\frac{u_L''}{u_L'}\Big)\frac{1}{x_\tau^2}, \tag{44}$$

see (35) and (37). Substituting (41), (42) and (44) in the right-hand side of (43) one finds by algebra

$$-\eta_{0x}\bar{u}_1(\tau, \eta_0, t) + \bar{v}_1(\tau, \eta_0, t) = -\frac{5Q^3\mu^2}{u_L'}\frac{1}{x_\tau^8} + \frac{5}{6}Q^2\Big[Q\mu' + 7Q'\mu - 10Q\mu\frac{u_L''}{u_L'}\Big]\frac{1}{x_\tau^7} +$$

$$\Big[5a_4 Q\frac{u_L''}{u_L'} - (Qa_4)'\Big]\frac{1}{x_\tau^6} + \frac{2\mu Q C_1}{u_L'}\frac{1}{x_\tau^4} + \Big[2QC_1\frac{u_L''}{u_L'} - (QC_1)'\Big]\frac{1}{x_\tau^3} = \sum_{n=3}^{8}\frac{D_n(\tau)}{x_\tau^n(\tau, t)}. \tag{45}$$

The differential equation (43) with the right-hand side (45) is solved using (40) in the same way as the equation (38) has been solved. The resulting formula reads

$$\bar{\eta}_1(\tau, t) = -\sum_{n=3}^{8}\frac{D_n(\tau)}{u_L'(\tau)(n-2)x_\tau^{n-1}(\tau, t)} + \frac{C_2(\tau)}{x_\tau(\tau, t)}, \tag{46}$$

where the coefficients $D_n(\tau)$ are introduced in (45), and $C_2(\tau)$ is to be determined using the condition $\bar{\eta}_1(\tau, \tau) = 0$, see (28).

The second-order terms of the flow velocity components (41), (42) and the free-surface elevation (46) are finite everywhere in the wake except of the position $x = x_*$ and time $t = t_*$, where and when the derivative $x_\tau(\tau, t)$ is zero. The second-order terms are singular at $x = x_*$ and $t = t_*$ and their orders of singularity are higher than those of the corresponding leading order terms. For example, the leading order elevation of the free surface, $\overline{\eta}_0(\tau, t) = Q(\tau)/x_\tau(\tau, t)$, see (35), increases as $O(x_\tau^{-1})$ when $x_\tau \to 0$, but the second-order elevation $\overline{\eta}_1(\tau, t)$ increases as $O(x_\tau^{-7})$. Therefore, the obtained second-order solutions in the wake are not valid near $x = x_*$ and $t = t_*$, where an inner solution should be derived, in order to obtain the uniformly valid asymptotic solution of the original problem as $\varepsilon \to 0$. To formulate the inner problem, we need to determine the scales of the inner variables and unknown functions in terms of ε. We assume that the scales of the inner variables are the same as the scales of the original outer variables where $x \to x_*$ and $t \to t_*$, which guarantee that the leading order terms and the second-order terms in the asymptotic expansions (22) are of the same order as $\varepsilon \to 0$. Note that the second order hydrodynamic pressure $p_1(x, y, t)$ also can be obtained analytically solving the problem (29). However, the function $p_1(x, y, t)$ will be not required to formulate the inner problem describing local flow near the singularity of the outer solution.

V. SINGULARITY OF THE OUTER SOLUTION

The leading-order solution obtained in section III becomes unbounded if $u_R(\tau) > 0$ and $u_L'(\tau) < 0$ for some values of the parameter τ. For such values of τ, the vertical flow velocity, $\bar{v}_0(\tau, y, t) = -yu_L'(\tau)/x_\tau(\tau, t)$, the free-surface elevation (35) and the hydrodynamic pressure (36) are singular at $t = t_c(\tau)$, where $x_\tau(\tau, t_c(\tau)) = 0$. This singularity occurs for the first time then, when $t_c(\tau)$ is minimum. If $t_c(\tau)$ is minimum at τ_*, then $t_c'(\tau_*) = 0$, $t_c''(\tau_*) > 0$ and $x_\tau(\tau_*, t_*) = 0$.

Differentiating equality $x_\tau(\tau, t_c(\tau)) = 0$ with respect to τ, setting $\tau = \tau_*$, and using that $t'_c(\tau_*) = 0$, we find $x_{\tau\tau}(\tau_*, t_*) = 0$. Differentiating $x_\tau(\tau, t_c(\tau)) = 0$ second time with respect to τ, setting $\tau = \tau_*$, and using inequalities $x_{\tau t}(\tau_*, t_*) = u'_L(\tau_*) < 0$ and $t'_c(\tau_*) > 0$, we obtain $x_{\tau\tau\tau}(\tau_*, t_*) > 0$. Note that $\partial^n x/\partial t^n = 0$ for $n \geq 2$. Using the obtained values of the derivatives at $\tau = \tau_*$ and $t = t_*$, one can approximate the function $x(\tau, t)$ and the derivative $x_\tau(\tau, t)$ near $\tau = \tau_*$ and $t = t_*$ by their Taylor series,

$$x(\tau, t) = x_* + u^*_L(t - t_*) + u^*_{L\tau}(t - t_*)(\tau - \tau_*) + \frac{1}{2}u^*_{L\tau\tau}(t - t_*)(\tau - \tau_*)^2 +$$

$$+\frac{1}{6}x^*_{\tau\tau\tau}(\tau - \tau_*)^3 + O(|\tau - \tau_*|^4) + O(|\tau - \tau_*|^3(t - t_*)),$$

$$x_\tau(\tau, t) = u^*_{L\tau}(t-t_*) + \frac{1}{2}x^*_{\tau\tau\tau}(\tau-\tau_*)^2 + u^*_{L\tau\tau}(\tau-\tau_*)(t-t_*) + O(|\tau-\tau_*|^3) + O(|\tau-\tau_*|^2(t-t_*)), \quad (47)$$

where the superscript $*$ means that the corresponding function is calculated at $t = t_*$ and $\tau = \tau_*$. For example $x^*_{\tau\tau\tau} = x_{\tau\tau\tau}(\tau_*, t_*)$. Note that $t < t_*$ in this section.

Applying the method of dominant balance to equations (47) where $t \to t_*$ and $\tau \to \tau_*$, we find that it is convenient to introduce local variables $\widetilde{\tau}$, $\widetilde{t}$, $\widetilde{x}$ and $\widetilde{y}$ by

$$\tau = \tau_* + \sigma\widetilde{\tau}, \quad t = t_* + \sigma^2\widetilde{t}, \quad x = x_* + u^*_L(t - t_*) + \sigma^3\widetilde{x}, \quad y = \sigma^{-2}\widetilde{y}, \quad (48)$$

where σ is small, $\sigma \ll 1$, $\widetilde{\tau} = O(1)$, $\widetilde{t} = O(1)$ and $\widetilde{t} < 0$. The new small parameter σ can be dependent of the small parameter ε of the original formulation, see section II. Then the asymptotic formulae (47) provide

$$\widetilde{x} = \widetilde{\tau}\left[u^*_{L\tau}\widetilde{t} + \frac{1}{6}x^*_{\tau\tau\tau}\widetilde{\tau}^2\right] + O(\sigma), \qquad x_\tau(\tau, t) = \sigma^2\left[u^*_{L\tau}\widetilde{t} + \frac{1}{2}x^*_{\tau\tau\tau}\widetilde{\tau}^2\right] + O(\sigma^3). \quad (49)$$

Here $u^*_{L\tau} < 0$, $\widetilde{t} < 0$ and $x^*_{\tau\tau\tau} > 0$. Therefore, the expressions in the square brackets in (49) are positive. This implies, in particular, that the part of the wake on the right from the singularity $x = x_*$ corresponds to $\tau > \tau_*$, and the part on the left from singularity corresponds to $\tau < \tau_*$. In order to minimise the number of parameters in the local description of the flow near the singularity, the stretched variables denoted by hats are introduced by

$$\widetilde{\tau} = (-\widetilde{t})^{1/2}A\widehat{\tau}, \quad \widetilde{t} = C\widehat{t}, \quad \widetilde{x} = C^{3/2}B\widehat{x}, \quad \widetilde{y} = D\widehat{y}, \quad (50)$$

where the coefficients A and B in (50) are given by $A = (6|u^*_{L\tau}|/x^*_{\tau\tau\tau})^{1/2}$, $B = A|u^*_{L\tau}|$ and the coefficients C and D will be selected later. Introducing $X = \widehat{x}(-\widehat{t})^{-3/2}$, one can write the first equation in (49) as

$$X = \widehat{\tau}(1 + \widehat{\tau}^2), \quad (51)$$

in the leading order. Correspondingly, the second equation in (49) reads

$$x_\tau(\tau, t) = \sigma^2(-\widetilde{t})|u^*_{L\tau}|(1 + 3\widehat{\tau}^2) + O(\sigma^3) \quad (52)$$

in the new stretched variables (50). Note that equation (51) does not depend on any parameters of the problem, thanks to the selected values of the coefficients A and B.

We shall determine the behaviour of the solution (25) close to $x = x_*$ and $t = t_*$ as the small parameter σ tends to zero. This limit is equivalent to $t \to t_*$, $\tau \to \tau_*$, where $x_\tau(\tau, t) \to 0$. The functions $u_1(x, y, t)$, $v_1(x, y, t)$ and $\eta_1(x, t)$ are given by (41), (42), (45) and (46). They are presented by the sums of terms proportional to negative integer powers of $x_\tau(\tau, t)$ with coefficients dependent on τ and y. The asymptotic behaviours of these functions as $t \to t_*$ and $\tau \to \tau_*$ are provided by terms with highest powers of $x_\tau^{-n}(\tau, t)$. One should be careful with this asymptotic analysis because some coefficients of the highest powers could be zero as $\tau \to \tau_*$. Note that some coefficients in (41), (42), (45) and (46) contain $\mu(\tau)$ as a factor, where $\mu(\tau) \to 0$ as $\tau \to \tau_*$.

Indeed, equation (39), which defines the function $\mu(\tau)$, yields

$$\mu(\tau) = u_L'(\tau) x_{\tau\tau}(\tau, t) - u_L''(\tau) x_\tau(\tau, t).$$

The asymptotic formula for $x_\tau(\tau, t)$ as $\tau \to \tau_*$ and $t \to t_*$ is given by (47). The corresponding formula for $x_{\tau\tau}(\tau, t)$ is obtained by differentiating the asymptotic formula for $x_\tau(\tau, t)$ with respect to τ,

$$x_{\tau\tau}(\tau, t) = x_{\tau\tau\tau}^*(\tau - \tau_*) + u_{L\tau\tau}^*(t - t_*) + \ldots$$

Note that equations (48) provide that $x_\tau(\tau, t) = O(\sigma^2)$ and $x_{\tau\tau}(\tau, t) = O(\sigma)$ as $\sigma \to 0$. Therefore,

$$\mu(\tau) = u_L'(\tau_*) x_{\tau\tau\tau}(\tau_*, t_*)(\tau - \tau_*) + O(|\tau - \tau_*|^2),$$

and then

$$\frac{\mu(\tau)}{x_\tau(\tau, t)} = \frac{-|u_{L\tau}^*| x_{\tau\tau\tau}^* \sigma \widetilde{\tau} + O(\sigma^2)}{\sigma^2(-\widetilde{t})|u_{L\tau}^*|(1 + 3\widehat{\tau}^2) + O(\sigma^3)} \sim -\frac{1}{\sigma}\sqrt{6|u_{L\tau}^*| x_{\tau\tau\tau}^*}(-\widetilde{t})^{-\frac{1}{2}} \frac{\widehat{\tau}}{1 + 3\widehat{\tau}^2} \tag{53}$$

as $\tau \to \tau_*$ and $t \to t_*$.

Note that the vertical coordinate y is from zero on the bottom of the liquid layer to $\eta(x, t)$ on the liquid free surface, where $\eta(x, t)$ is of the order of $\eta_0(x, t))$ as $\varepsilon \to 0$ and $\overline{\eta}_0(\tau, t) = Q(\tau)/x_\tau(\tau, t)$, see (35). Using (52), we find

$$\overline{\eta}_0(\tau, t) \sim \frac{Q^*}{|u_{L\tau}^*|(1 + 3\widehat{\tau}^2)} \frac{1}{(-\widetilde{t})\sigma^2} \tag{54}$$

as $\sigma \to 0$. Equation (54) explains the scale of the vertical coordinate in (48) near the point of the singularity. Correspondingly, the leading-order vertical velocity, $v_0(x, y, t) = -y u_{0x}(x, t)$, behaves as

$$v_0(x, y, t) \sim \frac{D}{\sigma^4} \frac{\widehat{y}}{(-\widetilde{t})(1 + 3\widehat{\tau}^2)}, \tag{55}$$

where $\sigma \to 0$ and $\widetilde{t}$, $\widehat{\tau}$, $\widehat{y}$ are of order $O(1)$. The asymptotic formula (55) for the leading order vertical velocity of the flow in the wake and the formula (42) written for $\sigma \to 0$ provide the second-order vertical velocity, see (22), in the local stretched variables,

$$\bar{v}(\tau, y, t) \sim \frac{D}{\sigma^4 C} \frac{\widehat{y}}{(-\widehat{t})(1 + 3\widehat{\tau}^2)} \Big\{ 1 + \tag{56}$$

$$\frac{\varepsilon^2}{\sigma^{10}} \cdot \frac{x_{\tau\tau\tau}^* Q^{*2}}{6|u_{L\tau}^*|^5 C^5} \cdot \Big[\frac{6}{(-\widehat{t})^5} \frac{27\widehat{\tau}^2 - 1}{(1 + 3\widehat{\tau}^2)^6} + \frac{\widehat{y}^2}{(-\widehat{t})^3} \frac{1 - 15\widehat{\tau}^2}{(1 + 3\widehat{\tau}^2)^4} \cdot \Big(\frac{DC|u_{L\tau}^*|}{Q^*} \Big)^2 \Big] \Big\}$$

It is convenient to select the constants D and C such that

$$\frac{x_{\tau\tau\tau}^* Q^{*2}}{|u_{L\tau}^*|^5 C^5} = 6, \qquad \frac{DC|u_{L\tau}^*|}{Q^*} = 1,$$

which gives

$$C = (Q^{*2} x_{\tau\tau\tau}^*/6)^{1/5}/|u_{L\tau}^*|, \qquad D = (6Q^{*3}/x_{\tau\tau\tau}^*)^{1/5}. \tag{57}$$

The formula (56) indicates that the second-order term of the vertical velocity is of the same order as the leading order term near the singularity point if the small parameter σ, which describes the dimension of the local region around this point, is related to the small parameter of the problem ε by the relation $\sigma = \varepsilon^{1/5}$. The asymptotic formula (56) with such C, D and σ reads

$$\bar{v}(\tau, y, t) \sim \frac{U_{sc}}{\sigma^4} \frac{\widehat{y}}{(-\widehat{t})(1+3\widehat{\tau}^2)} \left\{ 1 + \frac{6}{(-\widehat{t})^5} \frac{27\widehat{\tau}^2 - 1}{(1+3\widehat{\tau}^2)^6} + \frac{\widehat{y}^2}{(-\widehat{t})^3} \frac{1 - 15\widehat{\tau}^2}{(1+3\widehat{\tau}^2)^4} \right\}, \tag{58}$$

where $U_{sc} = D/C$. It can be shown that $D/C = \sqrt{C}|u^*_{L\tau}|A$.

The local asymptotics of the vertical velocity (58) is written in the moving coordinate system, see (48), with the size of the inner region in the x-direction being of the order of $\varepsilon^{3/5}$ in the dimensionless variables. The time scale of the development of jetting is of the order of $\varepsilon^{2/5}$.

In the moving coordinate system (48), the leading order term of the horizontal velocity (32) is approximated as

$$u_0(x,t) = u_L(\tau) = u^*_L + u^*_{L\tau}(\tau - \tau_*) + O(|\tau - \tau_*|^2) = u^*_L - \sigma(\sqrt{C}|u^*_{L\tau}|A)\sqrt{-\widehat{t}}\widehat{\tau} + O(\sigma^2) =$$
$$u^*_L - \sigma U_{sc}\sqrt{-\widehat{t}}\widehat{\tau} + O(\sigma^2). \tag{59}$$

The asymptotic formula (59) for the leading order horizontal velocity of the flow in the wake and the formula (41) written for $\sigma \to 0$ provide the second-order horizontal velocity, see (22), in the local stretched variables,

$$u(x,y,t) \sim u^*_L - \sigma U_{sc}\sqrt{-\widehat{t}}\widehat{\tau} \left\{ 1 - \frac{6}{(-\widehat{t})^5(1+3\widehat{\tau}^2)^5} + \frac{3\widehat{y}^2}{(-\widehat{t})^3(1+3\widehat{\tau}^2)^3} \right\}, \tag{60}$$

where relation $\sigma = \varepsilon^{1/5}$ and the formulae (57) were used. The vertical velocity (58) is an even function of $\widehat{\tau}$ and the horizontal velocity (60) is an odd function of $\widehat{\tau}$. This implies that locally and in the leading order the flow near the singular point is symmetric with respect to $\widehat{x} = 0$.

The leading order shape of the free surface near the singular point is given by (54). The asymptotic formula for the second-order contribution to the free-surface elevation (46) in the local stretched variables as $\sigma \to 0$ provides the outer second-order elevation as

$$\eta(x,t) \sim \frac{1}{\sigma^2} \frac{D}{(-\widehat{t})(1+3\widehat{\tau}^2)} \left\{ 1 + \frac{27\widehat{\tau}^2 - 1}{(-\widehat{t})^5(1+3\widehat{\tau}^2)^6} \right\}. \tag{61}$$

This formula predicts that the second-order elevation is an even function of $\widehat{x}$, which tends to $+\infty$ as $\widehat{t} \to 0^-$, where $|\widehat{\tau}| > (27)^{-\frac{1}{2}}$ and to $-\infty$, where $|\widehat{\tau}| < (27)^{-\frac{1}{2}}$.

The performed asymptotic analysis and the obtained asymptotic formulae (58), (60) and (61) show that the leading order terms and and the second order terms of the vertical and horizontal velocities, as well as of the free-surface elevation, are of the same order near the singular point if $\sigma = O(\varepsilon^{1/5})$. This means that the size of the inner region close to the singular point in x-direction is $O(\varepsilon^{3/5})$. Inner variables should be introduced in the inner region. Then the asymptotic analysis should be performed in the inner region leading to the inner solution describing jet formation on the surface of the wake. The inner solution should be matched with the so-called inner limit of the outer solution , which is represented by equations (58), (60) and (61). It is reasonable to select the variables $\widehat{x}$, $\widehat{y}$, $\widehat{t}$, which were defined in this section, as the inner variables.

VI. EQUATIONS DESCRIBING THE INNER SOLUTION

The asymptotic behaviour of the outer solution near the singular point, which was derived in Section 5, suggests that the inner variables and unknown functions are convenient to be introduced as

$$x = x_* + u_L^*(t - t_*) + \sigma^3 D\widehat{x}, \qquad y = \sigma^{-2} D\widehat{y}, \qquad t = t_* + \sigma^2 C\widehat{t}, \qquad u = u_L^* + \sigma U_{sc}\widehat{u}(\widehat{x}, \widehat{y}, \widehat{t}, \sigma),$$

$$v = \sigma^{-4} U_{sc}\widehat{v}(\widehat{x}, \widehat{y}, \widehat{t}, \sigma), \qquad \eta = \sigma^{-2} D\widehat{\eta}(\widehat{x}, \widehat{t}, \sigma), \qquad p = \sigma^{-8} U_{sc}^2 \widehat{p}(\widehat{x}, \widehat{y}, \widehat{t}, \sigma), \tag{62}$$

where $\sigma = \varepsilon^{1/5}$, and the constants D, C and U_{sc} are defined in section V. Substituting (62) in the original equations of flow (17) and the boundary condition (18) and (19), we obtain

$$\frac{\widehat{D}\widehat{u}}{\widehat{D}\widehat{t}} = -\frac{\partial \widehat{p}}{\partial \widehat{x}}, \quad \frac{\widehat{D}\widehat{v}}{\widehat{D}\widehat{t}} = -\frac{\partial \widehat{p}}{\partial \widehat{y}}, \quad \frac{\partial \widehat{u}}{\partial \widehat{x}} + \frac{\partial \widehat{v}}{\partial \widehat{y}} = 0, \quad \frac{\partial \widehat{u}}{\partial \widehat{y}} - \frac{\partial \widehat{v}}{\partial \widehat{x}} = 0 \quad (0 < \widehat{y} < \widehat{\eta}(\widehat{x}, \widehat{t}), |\widehat{x}| < \infty), \tag{63}$$

$$\frac{\partial \widehat{\eta}}{\partial \widehat{t}} + \widehat{u}\frac{\partial \widehat{\eta}}{\partial \widehat{t}} = \widehat{v}, \quad \widehat{p} = 0 \quad (\widehat{y} = \widehat{\eta}(\widehat{x}, \widehat{t}), \quad |\widehat{x}| < \infty), \quad \widehat{v} = 0 \quad (\widehat{y} = 0, \quad |\widehat{x}| < \infty), \tag{64}$$

where $\frac{\widehat{D}}{\widehat{D}\widehat{t}} = \frac{\partial}{\partial \widehat{t}} + \widehat{u}\frac{\partial}{\partial \widehat{x}} + \widehat{v}\frac{\partial}{\partial \widehat{y}}$ is the material derivative written in the inner variables $\widehat{x}$, $\widehat{y}$ and $\widehat{t}$. The equations (63) imply that the inner flow is two-dimensional, non-linear, unsteady and irrotational. The hydrodynamic problem (63) and (64) with unknown in advance free surface $\widehat{y} = \widehat{\eta}(\widehat{x}, \widehat{t})$ is to be solved subject to the following conditions as $|\widehat{x}| \to \infty$ and $\widehat{t} \to -\infty$:

$$\widehat{u}(\widehat{x}, \widehat{y}, \widehat{t}) \sim -\sqrt{-\widehat{t}}\,\widehat{\tau} \left\{1 - \frac{6}{(-\widehat{t})^5(1 + 3\widehat{\tau}^2)^5} + \frac{3\widehat{y}^2}{(-\widehat{t})^3(1 + 3\widehat{\tau}^2)^3}\right\}, \tag{65}$$

$$\widehat{v}(\widehat{x}, \widehat{y}, \widehat{t}) \sim \frac{\widehat{y}}{(-\widehat{t})(1 + 3\widehat{\tau}^2)} \left\{1 + \frac{6}{(-\widehat{t})^5}\frac{27\widehat{\tau}^2 - 1}{(1 + 3\widehat{\tau}^2)^6} + \frac{\widehat{y}^2}{(-\widehat{t})^3}\frac{1 - 15\widehat{\tau}^2}{(1 + 3\widehat{\tau}^2)^4}\right\}, \tag{66}$$

$$\widehat{\eta}(\widehat{x}, \widehat{t}) \sim \frac{1}{(-\widehat{t})(1 + 3\widehat{\tau}^2)} \left\{1 + \frac{27\widehat{\tau}^2 - 1}{(-\widehat{t})^5(1 + 3\widehat{\tau}^2)^6}\right\}, \tag{67}$$

$$\widehat{p}(\widehat{x}, \widehat{y}, \widehat{t}) \sim \frac{1 - \widehat{y}^2\widehat{t}^2(1 + 3\widehat{\tau}^2)^2}{\widehat{t}^4(1 + 3\widehat{\tau}^2)^4}, \tag{68}$$

where $\widehat{\tau}$ is the solution of the equation

$$\frac{\widehat{x}}{(-\widehat{t})^{3/2}} = \widehat{\tau}(1 + \widehat{\tau}^2), \tag{69}$$

see (56), (60), (61) and (62). Note that there are no parameters in the equations of motion (63), the boundary conditions (64) and the far-field conditions (65) – (68). Therefore, the inner problem written in the stretched variables is universal. Application of this problem to a particular situation requires only corresponding stretching of the independent variables and the unknown functions. The problem (63) – (69) will be investigated numerically in Part 2 of this study.

Below we drop hats and denote the right-hand sides in (65)-(68) by $u_\infty(x, y, t)$, $v_\infty(x, y, t)$, $\eta_\infty(x, t)$ and $p_\infty(x, y, t)$ correspondingly. One can show by direct calculations that $u_\infty(x, y, t)$ and $v_\infty(x, y, t)$ satisfy the continuity equation in (63) exactly. The equation of zero vorticity is satisfied only approximately as $t \to -\infty$,

$$\frac{\partial u_\infty}{\partial y} - \frac{\partial v_\infty}{\partial x} = \frac{12y}{(-t)^{\frac{15}{2}}(1 + 3\tau^2)^7}\Big[6\frac{81\tau^2 - 8}{(1 + 3\tau^2)^2} + 5\tau y^3(1 - 6\tau^2)\Big], \tag{70}$$

where the right-hand side is small compared with each term on the left-hand side of this equation. For example, $\partial u_\infty/\partial y = -6\tau y(-t)^{-\frac{5}{2}}(1+3\tau^2)^3$. Higher-order terms in the conditions (65)-(68) can be obtained using the approach by Iafrati and Korobkin (2004), section IIB, Korobkin and Iafrati (2005), Section 5, and Korobkin, Khabakhpasheva Rodriguez-Rodriguez, J. (2017). Such asymptotic formulae are used to reduce the computational domains of non-linear potential flows with free surfaces.

The equations (63), boundary (64) and far-field (65)-(68) conditions predict that the flow is symmetric with respect to $x = 0$. Therefore, only the region $x > 0$ can be considered with the condition $u(0, y, t) = 0$ on the line of symmetry. The inner problem (63)-(68) can be formulated for a velocity potential $\Phi(x, y, t)$ as it is depicted in Fig. 3. The free-surface shape $\eta_\infty(x, t)$, the horizontal velocity of the flow $u_\infty(x, 0, t)$ and the pressure $p_\infty(x, 0, t)$ on the bottom of the liquid layer, $y = 0$, predicted by the far-field conditions (67), (65) and (68), are shown in Fig. 4*(a-c)* at different time instants and only for $x > 0$. It is seen how the vertical jet starts to build up. Note that $u_\infty(x, y, t) \sim -x^{1/3}$ and $\eta_\infty(x, t) \sim [(-t)+\rho x^{2/3}]^{-1}$ as $t \to -\infty$, $x \to +\infty$. Fig. 4 demonstrates that the elevation of the free surface in the inner region increases and becomes more localized in time. The pressure at the bottom of the liquid layer in the inner region sharply increases as well and also localizes in the let root. On the other hand, the horizontal speed of the flow in the jet root, see Fig.4(c), increases at a certain distance from the jet root and remains zero at the jet centre.

The dimensional scale of both the horizontal and vertical velocity components in the inner region is $U\varepsilon^{\frac{1}{5}}D/C$, where D and C are defined by (57). It is obtained by combining (11) and (62). The corresponding dimensional scales of the free-surface elevation and the hydrodynamic pressure in the inner region are $h\varepsilon^{-\frac{2}{5}}D$ and $\rho U^2\varepsilon^{\frac{2}{5}}(D/C)^2$.

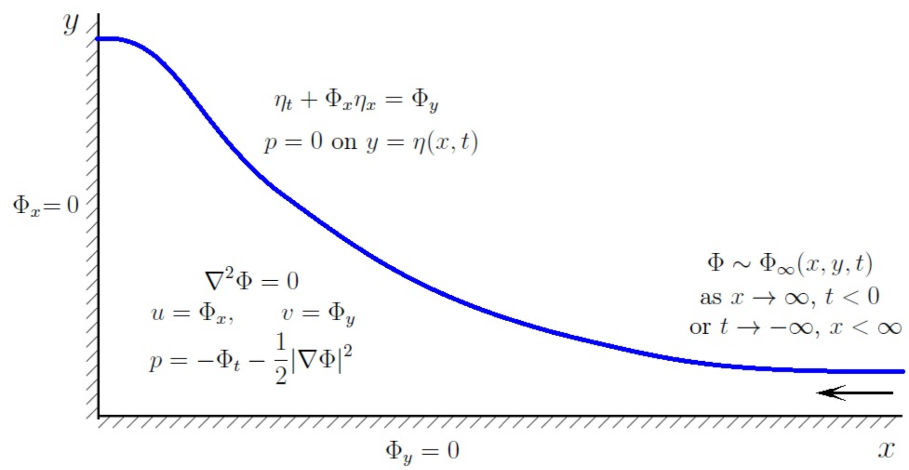

FIG. 3. Formulation of the inner problem (63)-(68) in terms of the velocity potential $\Phi(x, y, t)$. Asymptotic behaviours of this potential and the free-surface shape as $t \to -\infty$ are described by $\Phi_\infty(x, y, t)$, which is obtained from (65) and (66), and $\eta_\infty(x, t)$.

VII. CONCLUSION

The two-dimensional unsteady flow in a thin wake behind a plate obliquely impacting on a liquid layer was investigated by asymptotic methods. A small parameter of the problem ε is the ratio of the vertical and horizontal velocities of the flow at the entrance to the wake. Inertia dominated regime of the flow in the wake was studied. It was shown that gravity, surface tension and viscosity of the liquid can be neglected if the inflow velocity is relatively high. In the conditions of calculations done by Khabakhpasheva and Korobkin (2020a) for oblique impact by an elastic plate onto a thin liquid

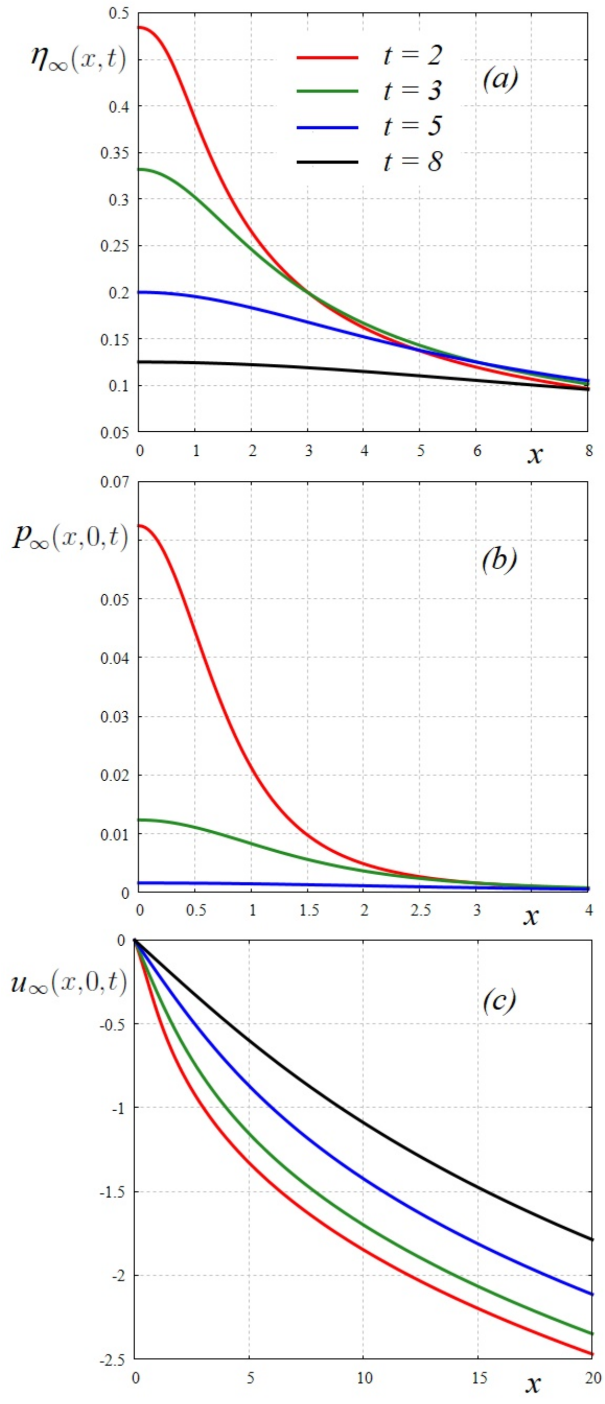

FIG. 4. The shape of the free surface $\eta_\infty(x,t)$ *(a)*, the pressure $p_\infty(x,0,t)$ *(b)* and the horizontal velocity $u_\infty(x,0,t)$ *(c)* along the bottom, $y = 0$, at different time instants $t = 8$ (black line), $t = 5$ (blue line), $t = 3$ (green line), $t = 2$ (red line) in dimensionless variables.

layer, the Weber and Reynolds numbers were of order 10^5 and the Froude number was of order of 10. Other regimes of the flows in a thin wake will be investigate in Part 3 of this work.

It was shown that acceleration of the flow into the wave leads to a gradient catastrophe, the time and place of which is predicted by the leading order solution. The thin layer approximation predicts unbounded growth of the wake thickness at the place of the catastrophe. The second-order outer solution of the original problem was obtained and its asymptotic behaviour when and where the catastrophe is approached was analysed. This analysis helped us to find the scales of the inner variables in terms of the small parameter ε and formulate the inner problem at the leading order. Appropriate moving coordinates were introduced for the inner problem. It was shown that the inner flow is two-dimensional, unsteady and potential. It is symmetric with respect to the origin of the inner coordinate system. The conditions of matching between the outer and inner solutions were obtained. These conditions provide the far-field conditions for the inner problem. The formulated inner problem will be solved numerically in Part 2 of this study. Preliminary results showed that the free-surface elevation and the hydrodynamic pressure increase at the centre of the inner flow and are getting localised near the jet root with time.

It was shown that the performed analysis can be applied to many practical problems, where influx into a thin liquid layer is accelerated with time. The present problem is two-dimensional. It would be interesting but very challenging to study the corresponding three-dimensional problem, where inflow into a thin liquid layer occurs through a time-dependent boundary with the normal and tangential inflow velocities being prescribed as functions of time and the position along the boundary.

AUTHORS' CONTRIBUTIONS

All authors contributed equally to this work.

ACKNOWLEDGMENTS

This work was supported by the Russian Science Foundation (Project No. 19-19-00287).

DATA AVAILABILITY

The data that support the findings of this study are available within the article.

APPENDIX A: BOUNDARY CONDITIONS ON THE FREE SURFACE OF THE LIQUID LAYER IN THE DIMENSIONLESS VARIABLES

The dynamic boundary conditions on the free surface, $y = \eta(x,t)$, are given by (5), where the stress tensor P is given by (6), the normal unit vector $\vec{n}$ and the tangent unit vector $\vec{\tau}$ to the free surface are given by (7), and the curvature of the free surface is æ $= \eta_{xx}/R^3$. We calculate

$$P\vec{n} = -\big(p + \rho g(h-\eta)\big)\vec{n} + \frac{2\rho\nu}{R}\Big(-\eta_x u_x + \frac{1}{2}(u_y+v_x),\ -\frac{1}{2}(u_y+v_x)\eta_x + v_y\Big) \qquad (A.1)$$

and then

$$\vec{\tau}\cdot P\vec{n} = \frac{2\rho\nu}{R^2}\Big((v_y-u_x)\eta_x + \frac{1}{2}(u_y+v_x)(1-\eta_x^2)\Big) = 0. \qquad (A.2)$$

In (A.2), $2\rho\nu/R^2 \neq 0$, $u_y = v_x - \omega$ from (2) and $v_y = -u_x$ from the continuity equation in (1).

Using these equalities, the boundary condition (A.2) provides

$$\omega = 2v_x - 4\frac{\eta_x u_x}{1-\eta_x^2}, \tag{A.3}$$

where

$$v_x = \frac{\partial v}{\partial x} = \frac{V\varepsilon}{h}\,\frac{\partial \tilde v}{\partial \tilde x}, \qquad \frac{\partial \eta}{\partial x} = \varepsilon \frac{\partial \tilde\eta}{\partial \tilde x}, \qquad u_x = \frac{\partial u}{\partial x} = \frac{U\varepsilon}{h}\,\frac{\partial \tilde u}{\partial \tilde x}, \qquad \omega = \frac{U}{h}\tilde\omega, \tag{A.4}$$

dimensionless variables are denoted by tilde, see (11) for the corresponding scales. Substituting (A.4) in (A.3) yields the second condition in (15).

Multiplying (A.1) by $\vec{n}$, we obtain the second condition in (5) in the form

$$-p - \rho g(h-\eta) + \frac{2\rho\nu}{R^2}\Big(\eta_x^2 u_x - \frac{1}{2}(u_y+v_x)\eta_x - \frac{1}{2}(u_y+v_x)\eta_x + v_y\Big) = \gamma\frac{\eta_{xx}}{R^3}. \tag{A.5}$$

By using $v_y = -u_x$, $u_y = v_x - \omega$ and (A.3), (A.4), we simplify the expression in the brackets in (A.5), which is related to the liquid viscosity, as

$$\eta_x^2 u_x - (u_y+v_x)\eta_x + v_y = u_x(\eta_x^2-1) - (2v_x-\omega)\eta_x = -u_x(1-\eta_x^2) - 4\frac{\eta_x^2 u_x}{1-\eta_x^2} =$$

$$= -\frac{u_x}{1-\eta_x^2}\Big((1-\eta_x^2)^2 + 4\eta_x^2\Big) = -u_x\frac{(1+\eta_x^2)^2}{1-\eta_x^2} = -\frac{U\varepsilon}{h}\,\frac{\partial \tilde u}{\partial \tilde x}\,\frac{\tilde R_+^4}{\tilde R_-^2} \tag{A.6}$$

in the dimensionless variables (11). Condition (A.5) in the dimensionless variables with account for (A.6) reads

$$-\rho V^2\tilde p - \rho g h(1-\tilde\eta) - 2\,\frac{\rho\nu}{h}\,\frac{U\varepsilon}{\tilde R_+^2}\,\frac{\partial \tilde u}{\partial \tilde x}\,\frac{\tilde R_+^4}{\tilde R_-^2} = \frac{\gamma\varepsilon^2}{h}\,\frac{\tilde\eta_{\tilde x\tilde x}}{\tilde R_+^3}. \tag{A.7}$$

Dividing both sides of (A.7) by ρV^2, we obtain

$$\tilde p(\tilde x, \tilde\eta(\tilde x, \tilde t), \tilde t) = \frac{gh}{V^2}(\tilde\eta - 1) - \frac{\gamma\varepsilon^2}{h\rho V^2}\,\frac{1}{\tilde R_+^3}\,\frac{\partial^2\tilde\eta}{\partial \tilde x^2} - 2\,\frac{\nu\varepsilon U}{hV^2}\,\frac{\partial \tilde u}{\partial \tilde x}\,\frac{\tilde R_+^2}{\tilde R_-^2}, \tag{A.8}$$

where $\varepsilon = V/U$, $gh/V^2 = 1/Fr^2$, $\gamma\varepsilon^2/(\rho h V^2) = \gamma/(\rho h U^2) = 1/We$, $\nu\varepsilon U/(hV^2) = \nu V/(hV^2) = \nu/(hV) = 1/Re$. The Froude number Fr, the Weber number We, and the Reynolds number Re are introduced in section II. The condition (A.8) yields the condition (16).

The first condition in (15) is the kinematic boundary condition (4) written in the dimensionless variables (11).

APPENDIX B: EQUATION (23)-(30)

Substituting asymptotic expansions (22) in equations (17) and collecting terms of the same order in ε as $\varepsilon \to 0$, we obtain

$$\frac{\partial u_0}{\partial t} + u_0\frac{\partial u_0}{\partial x} + v_0\frac{\partial u_0}{\partial y} + \varepsilon^2\left[\frac{\partial u_1}{\partial t} + u_1\frac{\partial u_0}{\partial x} + u_0\frac{\partial u_1}{\partial x} + v_1\frac{\partial u_0}{\partial y} + v_0\frac{\partial u_1}{\partial y} + \frac{\partial p_0}{\partial x}\right] = O(\varepsilon^4), \tag{B.1}$$

$$\frac{\partial v_0}{\partial t} + u_0\frac{\partial v_0}{\partial x} + v_0\frac{\partial v_0}{\partial y} + \frac{\partial p_0}{\partial y} + \varepsilon^2\left[\frac{\partial v_1}{\partial t} + u_1\frac{\partial v_0}{\partial x} + u_0\frac{\partial v_1}{\partial x} + v_1\frac{\partial v_0}{\partial y} + v_0\frac{\partial v_1}{\partial y} + \frac{\partial p_1}{\partial y}\right] = O(\varepsilon^4), \tag{B.2}$$

$$\frac{\partial u_0}{\partial x}+\frac{\partial v_0}{\partial y}+\varepsilon^2\left[\frac{\partial u_1}{\partial x}+\frac{\partial v_1}{\partial y}\right]=O(\varepsilon^4), \tag{B.3}$$

$$\frac{\partial u_0}{\partial y}+\varepsilon^2\left[\frac{\partial u_1}{\partial y}-\frac{\partial v_0}{\partial x}\right]=O(\varepsilon^4). \tag{B.4}$$

Equation (B.4) in the leading order as $\varepsilon \to 0$ provides $\partial u_0/\partial y = 0$. This equality together with the leading order equation (B.1) gives the first equation in (23), $u_{0t} + u_0 u_{0x} = 0$. The second equation in (23) is the leading order of (B.3), $v_{0y} = -u_{0x}$. The leading order equation (B.2) provides now the following equation for the leading order hydrodynamic pressure in the wake,

$$-p_{0y} = v_{0t} + u_0 v_{0x} - v_0 u_{0x}. \tag{B.5}$$

The terms of order $O(\varepsilon^2)$ in (B.1)-(B.4) provide the following equations for the first-order terms in (22):

$$u_{1t} + u_0 u_{1x} + u_1 u_{0x} + v_0 u_{1y} = -p_{0x}, \tag{B.6}$$

which is equation (26), where we used that $u_{0y} = 0$,

$$-p_{1y} = v_{1t} + u_0 v_{1x} + u_1 v_{0x} + v_0 v_{1y} + v_1 v_{0y}, \tag{B.7}$$

which is equation (29),

$$v_{1y} = -u_{1x}, \tag{B.8}$$

which is equation (27), and

$$u_{1y} = v_{0x}, \tag{B.9}$$

which is equation (30).

Taylor series for functions on the free surface, for example,

$$v(x,\eta(x,t),t) = v(x,\eta_0(x,t),t) + v_y(x,\eta_0(x,t),t)\big(\eta(x,t)-\eta_0(x,t)\big) + O\big[(\eta-\eta_0)^2\big],$$

and the asymptotic expansions (22) are used to derive the kinematic and dynamic boundary conditions (18) on the free surface. We obtain

$$v(x,\eta(x,t),t) = v_0(x,\eta_0,t) + \varepsilon^2\big[v_1(x,\eta_0,t) + \eta_1 v_{0y}(x,\eta_0,t)\big] + O(\varepsilon^4), \tag{B.10}$$

$$u(x,\eta(x,t),t) = u_0(x,t) + O(\varepsilon^2), \tag{B.11}$$

$$p(x,\eta(x,t),t) = p_0(x,\eta_0,t) + \varepsilon^2\big[p_1(x,\eta_0,t) + \eta_1 p_{0y}(x,\eta_0,t)\big] + O(\varepsilon^4). \tag{B.12}$$

Substituting (22), (B.10)-(B12) in the kinematic condition (18) and collecting terms of the same order as $\varepsilon \to 0$, we find

$$\eta_{0t} + \eta_{0x} u_0 + \eta_0 u_{0x} + \varepsilon^2\big[\eta_{1t} + \eta_{1x} u_0 + \eta_1 u_{0x} - v_{0y}\eta_1 - v_1\big] = O(\varepsilon^4). \tag{B.13}$$

Correspondingly, the dynamic boundary condition, $p = 0$ on $y = \eta(x,t)$, in (18) yields

$$p_0 + \varepsilon^2\big[p_1 + p_{0y}\eta_1\big] = O(\varepsilon^4), \tag{B.14}$$

which gives the boundary conditions in (25) and (29). The functions in (B.13) and (B.14) are calculated at $y = \eta_0(x,t)$.

The boundary conditions on the bottom of the liquid layer (19) gives the boundary conditions $v_0(x,0,t) = 0$ in (23) and $v_1(x,0,t) = 0$ in (27). Substituting expansions (22) in the conditions at

$x = L(t)$, we obtain the condition $u_0(L(t), t) = u_L(t)$ in (23) because $u_0(x, t)$ is independent of y, and the conditions in (24), (26) and (28).

The equation $v_{0y} = -u_{0x}$ in (23) and the condition $v_0(x, 0, t) = 0$ give $v_0(x, y, t) = -yu_{0x}(x, t)$. Substituting this equation in (B.13) we obtain the equation (24) in the leading order and equation (28) for $\eta_1(x, t)$ in the first order as $\varepsilon \to 0$.

Finally substituting $v_0 = -yu_{0x}$ in (B.5), we calculate

$$-p_{0y} = -yu_{0xt} - yu_0u_{0xx} + yu_{0x}^2 = -y(u_{0t} + u_0u_{0x})_x + yu_{0x}^2 + yu_{0x}^2 = 2yu_{0x}^2, \qquad (B.15)$$

where we used equation $u_{0t} + u_0u_{0x} = 0$ from (23). Equation (B.15) provides equation (25).

REFERENCES

Bukreev, V. I, Gusev, A. V., "Gravity waves generated by a body falling onto shallow water," J. Appl. Mech. Tech. Phys. **37**(2), 224-231 (1996).

Cherdantsev, A. V., Hann, D. B., Hewakandamby, B. N., Azzopardi, B. J., "Study of the impacts of droplets deposited from the gas core onto a gas-sheared liquid film," Int. J. of Multiphase Flow **88**, 69-86 (2017).

Edwards, C. M., Howison, S. D., Ockendon, H., Ockendon, J. R. "Non-classical shallow water flows,"IMA journal of applied mathematics, **73**(1), 137-157 (2008).

Faltinsen, O. M., Semenov, Y. A. The effect of gravity and cavitation on a hydrofoil near the free surface. J. Fluid Mech. **597**, 371-394 (2008).

Hann, D. B., Cherdantsev A. V., Azzopardi, B. J., "Study of bubbles entrapped into a gas-sheared liquid film," Int. J. of Multiphase Flow, **108**, 181-201 (2018).

Hicks, P. D., Purvis, R., "Air cushioning and bubble entrapment in three-dimensional droplet impacts," J. Fluid Mech. **649**, 135-163 (2010).

Hicks, P. D., Purvis, R., "Air cushioning in droplet impacts with liquid layers and other droplets," Phys. Fluids **23**(6), 062104 (2011).

Iafrati, A., Korobkin, A. A., "Initial stage of flat plate impact onto liquid free surface," Phys. Fluids, **16**(7), 2214-2227 (2004).

Kang, H. D., Oh, S. H., Kwon, S. H., Chung, J. Y., Jung, K. H., Jo, H. J., "An experimental study of shallow water impact," In *Proc. 23rd Int. Workshop on Water Waves and Floating Bodies.* (2008).

Khabakhpasheva, T. I., Korobkin, A. A., "Liquid drop impact on a vibrating substrate, " in *Proc. 3rd Int. Conf. Violent Flows (VF-2016), Osaka, Japan, 9-11 March* (2016).

Khabakhpasheva, T. I., Korobkin, A. A., "Oblique elastic plate impact on thin liquid layer," Phys. Fluids **32**(6), 062101 (2020a).

Khabakhpasheva, T. I., Korobkin, A. A. “Splashing of liquid droplet on a vibrating substrate,” Phys. Fluids, **32**(12), 122109 (2020b).

Korobkin, A. A., “Liquid-Solid Impact,” Siberian Branch of the Russian Academy of Sciences, Novosibirsk, (In Russian) (1997).

Korobkin, A. “Shallow-water impact problems,” J Eng. Math. **35**(1), 233-250 (1999).

Korobkin, A. A., Iafrati, A., “Hydrodynamic loads during initial stage of floating body impact,” J. Fluids Struct. **21**(4), 413-427 (2005).

Korobkin, A., Khabakhpasheva, T., Rodriguez-Rodriguez, J., “Initial stage of plate lifting from a water surface,” J. Eng. Math. **102**(1), 117-130 (2017).

Martinez-Legazpi, P., Rodriguez-Rodriguez, J., Korobkin, A., Lasheras, J. C., “Formation of corner waves in the wake of a partially submerged bluff body,” J. Fluid Mech. **771**, 547-563 (2015).

Meier, G. E. A., Klöpper, A., Grabitz, G., “The influence of kinematic waves on jet break down,” Exp. in fluids, **12**(3), 173-180 (1992).

Pegg, M., Purvis, R., Korobkin, A. A., “Droplet impact onto an elastic plate: A new mechanism for splashing,” J. Fluid Mech. **839**, 561 (2018).

Semenov, Y., Wu, G., “The nonlinear problem of a gliding body with gravity,” J. Fluid Mech. **727**, 132-160 (2013).

Shishmarev, K.A., Khabakhpasheva, T.I., Korobkin, A.A., “Free-surface flow behind elastic plate impacting on a thin liquid layer,” J. of Phys.: Conf. Series **1666**(1), 012059 (2020).

Stumpf, B., Roisman, I. V., Tropea, C., Hussong, J., Yarin, A. L., “Drop Impact onto a Thin Viscous Film: Corona Thickness Measurements,” In *Int. Conf. on Liquid Atomization and Spray Systems (ICLASS)* **1**(1) (2021).

Tong, R. P., Schiffers, W. P., Shaw, S. J., Blake, J. R., Emmony, D. C., “The role of ’splashing’ in the collapse of a laser-generated cavity near a rigid boundary,” J. Fluid Mech. **380**, 339-361. (1999).

Yarin, A. L. and Weiss, D. A. “Impact of drops on solid surfaces: self-similar capillary waves, and splashing as a new type of kinematic discontinuity,” J. Fluid Mech. **283**, 141-173 (1995).

Yoon, B. S., Semenov, Y. A., “Separated inviscid sheet flows,” J. Fluid Mech. **678**, 511-534 (2011).